Structure of Cerebrosides
I. Phrenosine at 23 °C and 66 °C

S. Fernandez-Bermudez, J. Loboda-Čačković, H. Čačković, and R. Hosemann

Fritz-Haber-Institut der Max-Planck-Gesellschaft, Teilinstitut für Strukturforschung, Berlin

(Z. Naturforsch. **32 c**, 362–374 [1977]; received February 16, 1977)

Glycosphingolipids, Biologic Membranstructures, Combined Small and Wide Angle X-Ray Analysis, Microparacrystallites

Small angle and wide angle powder diffraction diagrams (SAXS and WAXS) have been obtained from samples of dry phrenosine cerebrosides prepared from beef brain. Two kinds of lamellae bundles exist within the powder at 23 °C. The first (structure I) with 15% of the molecules having a long period P of 65 Å and a paracrystalline g-value (Hosemann and Bagchi [1962]) of 4.2% consists of orthorhombic subcells similar to C_nH_{2n+2} ($n \geqq 26$) buth with larger lateral dimensions. It has an angle of 60° between the chain direction and the lamellae surface which is parallel to the (201) netplanes of the paraffin-like subcells. The second (structure II) constitutes 22% of these lamellae and 63% with a period of 49 Å and triclinic subcells similar to $C_{20}H_{42}$. The angle between the chain direction and lamellae surface is here 45°. The SAXS reflections of structure II are analysed with a bimodal statistic which proves that the 65 Å and 49 Å lamellae are mixed statistically. At 66 °C only a structure III exists with a 52 Å long periodicity. Here all orthorhombic lamellae are built in but now their (301) netplanes are parallel to the lamellae surface. They obviously stabilize the structure instead of the (201)-netplanes which stabilize at 23 °C. A Fourier-analysis of the first 4 SAXS reflections of the relatively undistorted structures II and III projected to the normal of the lamellae surface shows a series of 21 Å wide step functions with a periodicity of 51 or 52 Å. This proves directly a head to head and teil to tail structure. The 21 Å wide heads are attributed to two galactose rings with their amide linkages and oxygens of the fatty acids and sphingosines. Knowing their size (9 Å) one unequivocally can phase the other 6 SAXS reflections which give rise to a gap of some Å's thick between them. The gap is deeper for structure II because here lamellae of two different thicknesses are mixed. Two further small gaps in the center of the bilayers indicate the ends of the double chain molecules. From the line widths of WAXS it is evident that small paracrystallites (mPC's) exist with 40 to 100 Å lateral dimensions. From SAXS line widths one concludes that bundles of 4 to 7 bilayers build up macroparacrystallites (MPC's), where each bilayer consists of 10 to 25 mPC's. Obviously the galactose rings on the surface of the bilayers produce much larger paracrystalline distortions than the methyl-end-groups in paraffins but much smaller ones than the backfolds in mats of polyethylene single crystals. Consequently 4 to 7 lamellae can be found in each MPC. The galactose rings are the cause of larger lateral distances between the paraffin-like chains and generate distortions corresponding to a g-value of ~2.6% in the mPC's. This is explained by the high degree of conformational variety that the chains adopt which is larger than in synthetic polyethylene. This would further explain why all our attempts to obtain better crystallinity failed.

I. Introduction

In recent years there have been an increasing number of investigations dealing with the analysis of biological membranes and their lipid model systems by X-ray diffraction methods [1–9]. In the present paper we wish to extend these studies to the case of beef brain cerebrosides which are one of the main components of specific tissues [10] and frequently related to antigenic properties [11]. Cerebrosides are a special type of glycosphingolipids with a lipophilic-component (ceramide, which is a long-chain fatty acid attached through an amide-linkage to a molecule of sphingosine – a long-chain base) and a carbohydrate residue (galactose) [12]. Their chemical constitution is illustrated in Fig. 1. The length of the long-chain fatty acid in beef as well as in human brain cerebrosides may vary between 14 and 27 carbon atoms [13, 14]. Studies of physical (optical and electrical) properties of bilayers of natural cerebrosides relating to the crystal-liquid crystal transitions have been recently reported [15]. X-ray diffraction studies of cerebrosides are, however, limited so far to the analysis of long spacings of crystalline phases and thermotropic and acqueous mesophases for natural samples with only one paraffin-like chain [16] and synthetic products [17] which have two such chains, but of equal length.

Requests for reprints should be sent to Prof. Dr. Dr. R. Hosemann, Teilinstitut für Strukturforschung, Fritz-Haber-Institut der Max-Planck-Gesellschaft, Faradayweg 4–6, *D-1000 Berlin 33.*

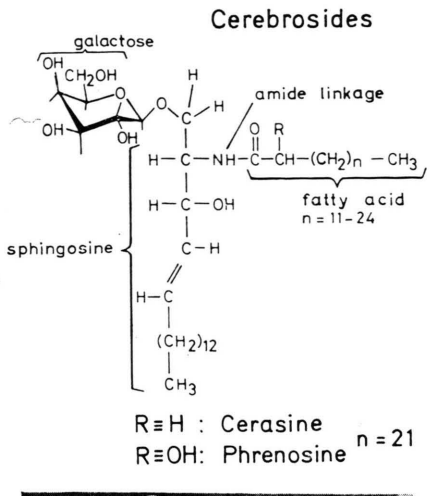

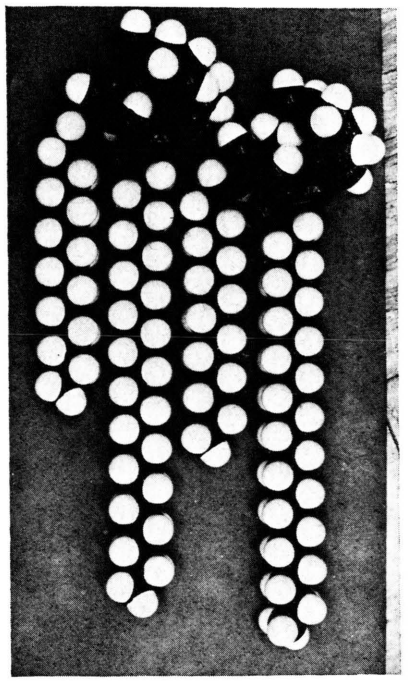

Fig. 1. Chemical constitution and calotte model of the subcell with triclinic cerebrosides. Conformational distortions of the chain are not introduced for simplicity.

In the present work we report on X-ray diffraction study of dry phrenosine. Phrenosine is the cerebroside with a fatty acid chain having 24 carbon atoms and a sphingosine having 18 carbon atoms. Phrenosine is, in fact, the major component (about 30%) of the acid in the natural samples [13, 14]. The main feature of our samples was their purity which was 95%. The purpose of this paper is to analyse the X-ray small angle (SAXS) and wide angle (WAXS) patterns of the unoriented material at 23 °C and 66 °C. Sample preparation and X-ray techniques are described in section II. SAXS at 23 °C of structure I and II can be found in section III and IV and at 66 °C in section V. From this one obtains direct information of the size of the lamellae bundles (MPC's), the thickness and packing arrangement of the lamellae which are bilayers of parallel aligned molecules. In section VI the projection of the electron density is calculated by Fourier-methods from one double molecule of a bilayer to the lamella normal of structure II and III. From WAXS data one obtains direct information on the molecular arrangement in these structures (section VII). In the last section we discuss the size and the distortions of the molecular lattice. It consists of 40 to 100 Å large microparacrystals (mPC's) which aggregate to the lamellae bundles (MPC's).

II. Experimental

Phrenosine was prepared from beef brain by Martin-Lomas and Chapman [12] after the method of Carter *et al.* [18]. By gas chromatographic analysis it was found that the sugar moiety is 100% galactose, the fatty acid residue corresponds in 95% to 2-hydroxy-*n*-tetracosanoic acid and the sphingosine residue at least 93% as indicated in Fig. 1. All attempts to obtain large enough crystals to get X-ray single crystal patterns or only partially oriented samples were without success. The X-ray pattern always consisted of Debye-rings. The sample remains in a non-crstalline state which has been described by the paracrystalline theory [19].

The powder samples were placed in Mark-capillaries of 1 mm diameter. SAXS patterns were produced from a Kiessig-camera with pinhole collimating and sample to film distances 182 mm or 382 mm. A Rigaku-Denki (5 kW) rotating anode X-ray generator was used to produce Cu Kα radiation. The first order SAXS reflections needed an exposure of 2 hours and the higher order 120 hours (Fig. 2). WAXS patterns were obtained in a Guinier-Jagodzinski camera of AEG-Telefunken which was calibrated with a $CaWO_4$ standard sample with crystallites larger than the resolution of the camera (1500 Å) and provided with a special sample holder for constant elevated temperatures of ± 1 °C constancy (built in our laboratory). Microdensitometer tracings of the SAXS and WAXS films were done with Joyce-Loebl equipment. Line profile analysis was performed after elimination of the col-

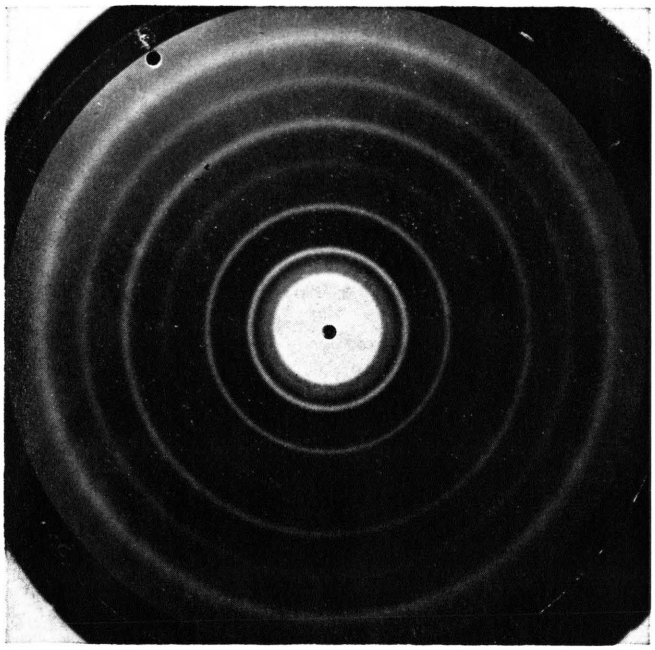

Fig. 2. SAXS of phrenosine at 23 °C. Sample to film distance 182 mm, CuKα-radiation.

limation error resolving the curves with a Du Pont 310 curve resolver. This was done for the SAXS by deconvoluting the experimental profile with that of the primary beam. The WAXS line width is influenced by the geometry of the camera, sample thickness, absorption and the monochromator quality. A correction was made by deconvoluting with a reflection from the $CaWO_4$ standard sample placed close to the sample. Then $CaWO_4$ powder was dispersed in atactic polystyrene in such a quantity and thickness that the absorption was the same as that of the sample. Finally the $\cos\vartheta$ correction was applied to discuss the intensities as functions of $b = 2\sin\vartheta/\lambda$.

III. SAXS at 23 °C of Structure I

In Fig. 2 a SAXS pattern is shown (exposure time 120 h), where the inner two Debye-rings are strongly overexposed. The microphotometer curve which leads to the intensity $I(b)$ must be multiplied by b^2 to eliminate for the effects of disorientation (Lorentz-factor). In Fig. 3 the $b^2 I(b)$-integral intensities of the SAXS reflections are plotted after elimination of the diffuse background. The thickness of the bars gives the experimental errors. The dashed reflections $n = 8$ and 9 are obtained from WAXS.

Two groups of SAXS-reflections exist. One containing three very diffuse and weak reflections with a basic period of ~ 65 Å (structure I) and one with nine relatively sharp reflections (structure II) and a lattice constant of 49 Å for $n > 2$, whereas the reflection $n = 1$ and 2 are somewhat shifted from their ideal positions to smaller b_n-values.

Structure I: The appearance of only 3 orders of reflections of the superlattice with a 65 Å periodicity P and their diffuse shape indicates that large distortions must exist int his lamellar bundles. As shown below, the lamellae are not packed together with full crystalline order. We have therefore called the bundles macroparacrystallites (MPC's). The paracrystalline distortions can be calculated as follows:

The integral widths δb of the reflections is plotted against the square of the order n ($n = b_n P$) of the reflections (Fig. 4). They lie on straight lines in structure II and obey the following rule from Hosemann and Bagchi [19].

$$\delta b = \frac{1}{D} + \frac{(\pi g n)^2}{P} \qquad (1)$$

where P is the macrolattice periodicity orthogonal to the lamellae and D is the mean size of the stacks of lamellae in the same direction. The paracrystalline distortion g of this macrolattice (MPC) is defined by the relative fluctuation of the lamellae distances P (from centre to centre)

$$g = \sqrt{\overline{P^2}/\overline{P}^2 - 1}\,. \qquad (2)$$

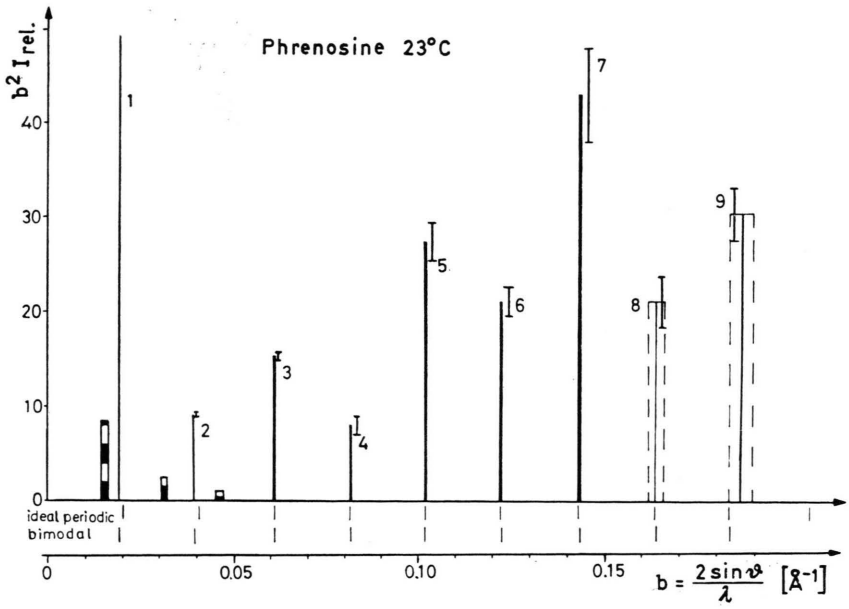

Fig. 3.
$b^2 I - b$-SAXS of phrenosine at 23 °C. The 3 reflections of structure I are indicated by black-white bars, those of structure II with the number n of higher orders. $n=8$ and 9 are obtained by WAXS.

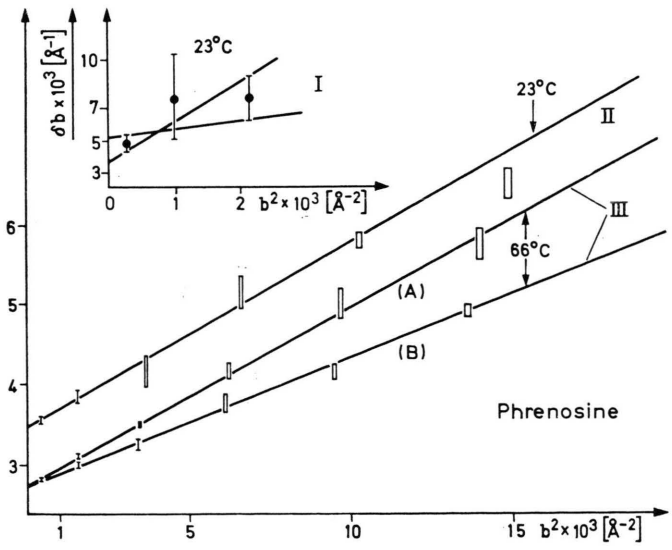

Fig. 4. $\delta b - b^2$ diagrams of the SAXS patterns of structure I, II and III. III(A) after 16 hours annealing at 66 °C and III(B) after 120 hours annealing at 66 °C.

This means that the lamellae are not periodically separated with a constant distance P. In structure I the measured δb-values have large error bars as shown in Fig. 4.I.

One obtains as a mean value between the two possible extreme straight lines and a mean error with the help of Eqn (1):

$$\begin{aligned} D &= (230 \pm 40)\ \text{Å}; \\ g &= (\ 4.2 \pm\ 2)\ \%; \\ P &= (\ 65 \pm\ 4)\ \text{Å}; \\ N &= D/P \sim 4\ \text{lamellae}. \end{aligned} \qquad (3)$$

IV. SAXS at 23 °C of Structure II

As mentioned above the experimentally found b_{exp}-values of the SAXS reflections of structure II are periodic only for $n \geqq 3$. They can be explained by a lattice constant $1/b_c = 49$ Å. The deviations from the b_{exp} are collected in Table I.

The displacement of the first two reflections from the ideal positions b_c can be explained by a so called "bimodal distance statistic" of the lamellae. This means that two different thicknesses of lamel-

n	b_{exp} [Å^{-1}] structure I	b_{exp} [Å^{-1}]	$(b_c - b_{exp}) \times 10^4$ structure II	$(b_c - b_n) \times 10^4$
1	0.0154	0.01926	11.1	11.0
2	0.0317	0.03937	13.6	13.6
3	0.0465	0.06093	1.7	−9
4		0.08161	−1.4	
5		0.10162	2.1	
6		0.12220	0.0	
7		0.14291	−3.4	
8		0.1620	9	
9		0.1823	10	

Table I. Position of the SAXS reflections of phrenosine at 23 °C. b_{exp} observed, b_c calculated with $c = 49$ Å, b_n calculated from Eqn (9).

lae exist and the corresponding two types of lamellae are statistically mixed within the bundle [20]. Let α be the statistical frequency of lamellae of the larger periodicity $(c+\delta)$ and $(1-\alpha)$ that of lamellae with c then the mean periodicity $\overline{P}$ is given by

$$\overline{P} = (1-\alpha)\cdot\overline{c} + \alpha(\overline{c}+\overline{\delta}) = \overline{c}(1+\alpha k)\,; \quad k = \overline{\delta}/\overline{c}\,. \tag{4}$$

Both types also vary in their thicknesses. If $H_0(x)$, $H_\delta(x)$ are the statistical distributions of their thicknesses x and

$$\begin{aligned} F_0(b) &= \int H_0(x+\overline{c})\, e^{-2\pi i b x}\, dx \\ F_\delta(b) &= \int H_\delta(x+\overline{c}+\overline{\delta})\, e^{-2\pi i b x}\, dx \end{aligned} \tag{5}$$

are the moduli of their Fourier-transforms then the complex vector

$$F(b) = F_0(1-\alpha)\, e^{-2\pi i \overline{c} b} + F_\delta\, \alpha\, e^{-2\pi i (\overline{c}+\overline{\delta}) b} \tag{6}$$

has to a first good approximation according to the theory of paracrystals maximum positive values at the position b_n of the maxima of the reflections, if

$$(1-\alpha) F_0(b_n) \sin 2\pi \overline{c}\, b_n + \alpha F_\delta(b_n) \cdot \sin 2\pi(\overline{c}+\overline{\delta}) b_n = 0\,. \tag{7}$$

Introducing $\sin(a+b) = \sin a \cos b + \cos a \sin b$ one obtains

$$\begin{aligned} \operatorname{tg} 2\pi b_n c &= \frac{\beta \sin 2\pi k b_n c}{1+\beta \cos 2\pi k b_n c}\,; \\ \beta &= \frac{\alpha F_\delta(b_n)}{(1-\alpha) F_0(b_n)}\,. \end{aligned} \tag{8}$$

For $k = 0$ or $\alpha = 0$, hence equally thick lamellae, one obtains the undistorted position $c\, b_c = n$ (n integer). Otherwise

$$\operatorname{tg} 2\pi (b_n - b_c) c = -\frac{\beta \sin 2\pi k n}{1+\beta \cos 2\pi k n} \tag{9}$$

defines the experimentally observed deviation $b_n - b_c$ from the ideal position b_c (Table I). As mentioned above for $c = 49$ Å all reflections $n \geqq 3$ lie within the error of experiment in the right position (see Table I). The reflections $n = 1$ and $n = 2$ lie at too small angles, hence correspond to thicker lamellae. Since their influence disappears at $n = 3$, we learn from structure I and from Eqns (5), (6), and (7) that the statistics H_δ of the thicker lamellae must have a larger statistical fluctuation in the order of 4% or more. Now for $n \geqq 3$ its Fourier-transform $F_\delta(b)$ can be neglected against F_0. Then $\beta = 0$ and the positions of all reflections with $n \geqq 3$ depend, according to Eqn (8) only on the structure with the smaller mean lamellae distance $\overline{c}$. From the slope of the straight line II in Fig. 4 and Eqn (1) one finds that the g_0-value of the 49 Å structure, if no larger $(c+\delta)$ lamellae would be mixed in, is

$$\overline{c} = 49 \text{ Å}; \quad g_0 = 2.2\%. \tag{10}$$

From the position of the reflections $n = 1$ and 2 one obtains with the help of Eqn (9) the two unknown quantities α and k, namely

$$\alpha = 0.26; \quad k = 0.22. \tag{11}$$

Hence, the second component has lamellae with a periodicity

$$\overline{c} + \overline{\delta} = 49 \text{ Å}(1+k) = (60 \pm 2) \text{ Å} \tag{12}$$

which agrees within the experimental errors with the value P of structure I in Eqn (3). The mean lamellar periodicity $\overline{P}$ of structure II is given by Eqn (4) and leads with the help of Eqn (11) to

$$\overline{P} = (52 \pm 1) \text{ Å}. \tag{13}$$

In structure II $\alpha = 26\%$ lamellae of structure I are statistically mixed with lamellae of 49 Å periodicity. The value $g = 4.2\%$ of structure I [Eqn (3)] nicely agrees with the fact that in structure II the reflections $n \geqq 3$ are no more influenced by the thicker lamellae, because the maximum number of reflections is given by $\sim 15/g(\%)$ according to the theory of paracrystals.

In Fig. 3 two positions of reflection are plotted on the bottom: Firstly of the 49 Å lattice, which agrees with all reflections $n \geqq 3$, and secondly the bimodal positions calculated from Eqn (9) with the values of Eqn (11).

The $\delta b - b^2$ diagram of structure II in Fig. 4 gives at the intersection with the ordinate according to Eqn (1) the value of the mean thickness D of the lamellae bundles. The average of $\overline{P^2}$ of the bundle is given by

$$\overline{P^2} = (1-\alpha)\overline{c^2}(1+g_0^2) + \alpha(\overline{c+\delta})^2(1+g_\delta^2)$$

and herefrom one obtains for the g-value of the MPC, mixed of two different lamellae types, according to Eqn (2): (14)

$$g^2 = \alpha(1-\alpha)\,\overline{\delta^2}/\overline{P^2} + \frac{(1-\alpha)g_0^2 + \alpha(1+k)^2 g_\delta^2}{(1+\alpha k)^2}$$

hence

$$\begin{aligned} g &= 10\%; \\ D &= 290\,\text{Å}; \\ \overline{P} &= 52\,\text{Å}; \\ N &\sim 6\ \text{lamellae}. \end{aligned} \qquad (15)$$

One obtains another interesting fact concerning the shape of MPC's (lamellae bundles) from the continuous SAXS at zero angle. The Guinier plot $\ln I$ *vs* b^2 of Fig. 5 can be separated into two Gaussian terms, the one with a radius of gyration 37 Å, the other with 96 Å. The latter corresponds to MPC's with a diameter $2\sqrt{5/3}\ 96\,\text{Å} = 248\,\text{Å}$

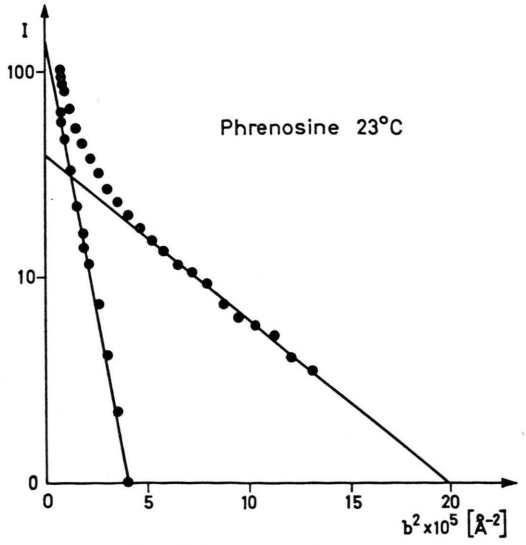

Fig. 5. Guinier-plot of the central SAXS peak of phrenosine at 23 °C. The outer tail gives information of the size of the mPC's and the inner tail of the MPC's.

averaged over all orientations. From Eqns (15) and (3) we learned that the extension of the MPC's orthogonal to the lamellae is 290 Å (structure II) and 230 Å (structure I). Herefrom one finds out that the lateral dimension of structure II must be somewhat smaller than 248 Å and that of structure I somewhat larger. The radius of gyration A of an uniaxial ellipsoid with the chief diameters D, B, B is given by

$$A^2 = \frac{1}{5}\left[\left(\frac{D}{2}\right)^2 + 2\left(\frac{B}{2}\right)^2\right]. \qquad (16)$$

Herefrom one obtains the mean lateral size of the bundle of lamellae

$$B = \begin{cases} 224\ \text{(structure II)} \\ 256\ \text{(structure I)}. \end{cases} \qquad (17)$$

The other Gaussian component of Fig. 5 indicates the existence of small units, the so called mPC's with a mean diameter of 95 Å, which build up the MPC's. Their sizes can be obtained also in more details from WAXS (see Table VI).

V. SAXS at 66 °C of Structure III

Fig. 6 gives similar to Fig. 3 the positions and integral intensities of the SAXS reflections at 66 °C. Besides one very diffuse (but not yet explained) reflection at 150 Å and one at 6.89 Å only one component with $P = 51$ Å is observable with ten higher orders. No bimodal effect exists (Table II). This structure III is obviously related to the 49 Å-component in the bimodal structure II discussed later.

In Fig. 4.III the $\delta b - b^2$ diagram of structure III is plotted. In curve (A) the sample was heated at 66 °C for 12 hours before making the exposure. In curve (B) the sample was heated additionally for 120 hours. The smaller slope of (B) indicates a decrease of the g-values of the MPC's by annealing which can be explained by a slow removing of defects from the MPC's. The result is

$$\begin{aligned} &\text{(A):}\quad D = 362\,\text{Å}; \quad g = 2.2\%; \quad N = 7. \\ &\text{(B):}\quad D = 362\,\text{Å}; \quad g = 1.8\%; \quad N = 7. \end{aligned} \qquad (18)$$

VI. Electron Density Projection of Structure II and III

We now calculate the projection of the electron density distribution $\varrho(x)$ on the lamellae normal using the SAXS integral intensities. We begin with

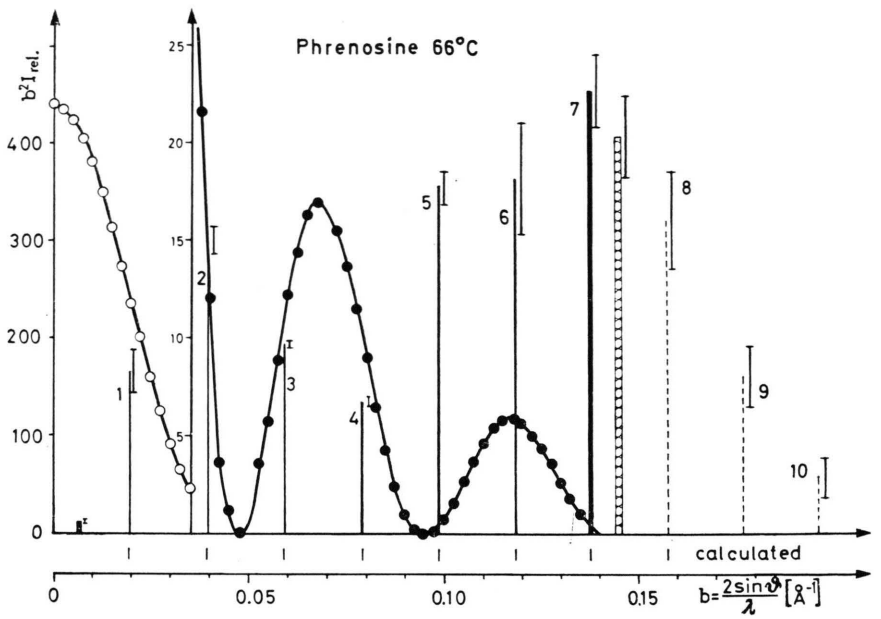

Fig. 6.
$b^2 I - b$-SAXS of phrenosine at 66 °C. The full line gives the structure factor of a step function [Eqn (20)] which gives the first information of the size of two adjacent galactose heads. The reflections 5 to 10 generate the gap in Fig. 7 between these adjacent galactose rings. The bars on top of the reflections represent the experimental error. The reflections 8, 9 and 10 are derived from the WAXS of Fig. 8. The reflection between that within $n=7$ and 8 cannot yet be explained.

b_{exp}[Å^{-1}]	d_{exp}[Å]	b_c[Å^{-1}]	P/n[Å]	$[b_{exp}-b_c]\times 10^4$
0.01964	50.91	0.01967	50.84	−0.3
0.03941	25.37	0.03935	25.41	0.6
0.05895	16.96	0.05902	16.94	−0.7
0.07892	12.67	0.07870	12.70	2.2
0.09844	10.15	0.09837	10.16	0.7
0.11823	8.45	0.11805	8.47	1.8
0.13772	7.26	0.13772	7.26	0.0
0.15750	6.35	0.15739	6.35	−1.1
0.17700	5.65	0.17706	5.64	0.6
0.19640	5.09	0.19674	5.08	3.4

Table II. Position of the SAXS reflections of phrenosine at 66 °C (structure III). b_{exp} observed, b_c calculated with $P=50.8$ Å.

structure III because of its larger simplicity. The open question is here the well known phase-problem of crystallography because we know only $I(b)$ which is the square of the amplitude. This phase-problem can be avoided, if one calculates the Fourier-inverstransformation of the whole intensity function and separates from this so called Q-function the Q_0-function of a single bilayer [19]. This is possible, if the number N of lamellae in one MPC is not too large. Lesslauer *et al.* [21] applied this method to bariumstearate with $N=2$. In our case N is too large and the resolution of the camera not good enough. So we have to find another way. Lesslauer *et al.* [21] analysed the structure of stearate also by Fourier-series with an experimentally established set of phases. The amplitude $b\sqrt{I(b)}$ is real when $\varrho(x)$ has a centre of symmetry and one has only to decide between + and − signs in the Fourier-coefficients $n\sqrt{I(n)}$:

$$\varrho(x)=\frac{2}{P}\sum_{n=1}^{N}\pm n\sqrt{I(n)}\cos 2\pi\frac{n}{P}x;\quad n=b_n P. \tag{19}$$

He adjusted the signs until $\varrho(x)$ was constant as well as possible in the region of the hydrocarbon chains.

Using the concept of convolution integrals [19] one can go a more direct way because $b^2 I(b)$ is the product of the squared Fourier-transform of one lamella with the lattice factor of the MPC. Since phrenosine has a larger electron density in the galactose rings together with the sphingosine part including the double bonded carbon atoms and the amide-linkage together with adjacent oxygens

(further on called "head") we start as a first approximation with a step function of the unknown extension L of these heads. The squared Fourier-transform of this step function is given by

$$\left(\frac{\sin \pi L b}{\pi b}\right)^2. \tag{20}$$

This function explains directly the $b^2 I(b)$-values of the first four reflections in Fig. 6, if we use

$$L = 21 \text{ Å}. \tag{21}$$

The size L and the distance $P - L$ between neighboured step functions proves directly that head to head and tail to tail packing occurs (Figs 9 and 10). Herefrom one learns that the structure amplitude $b\sqrt{I(b_n)} = \dfrac{\sin \pi L b_n}{\pi b_n}$ at $n = 1$ and 2 (continuous curve in Fig. 6) is positive and of $n = 3$ and 4 negative. Since its length L corresponds to two adjacent heads obviously an electron density gap must exist between the two heads. This can be generated by the reflections 5 to 10 which are only partially explained by the above mentioned shape function. The next intention is to avoid unnessary ripples produced by these reflections. Therefore we assigned to the reflections 5 to 10 of this group all the same phases. It now produces a highly damped cosine-wave. To decide the phase of this group we must ensure that a gap is generated in the middle of the $L = 21$ Å step function. This hence determines the signs of all the phases by placing its extreme negative value into the centre of the L-step. From Fig. 7 one learns that it is deeper for structure II at 23 °C. This may be caused by the fact that here often heads of the 45 Å and 65 Å lamellae touch each other which have different shapes (Figs 9 and 10). Moreover two small minima near the centre of the bilayer indicate the gaps between the endgroups of the two different long paraffin chains (see Fig. 1). Their distance of about 10 Å corresponds fairly well with the distance of the gaps between adjacent pairs of tails.

On the right hand side of Fig. 7 a scale is plotted which gives the values of the projection of the electron density $\varrho(x)$ of one double molecule calculated with the help of chemical data. The heads contain 178 electron. The hydrocarbon chain part of the fatty acid and of the sphingosine aligned parallel to each other contain 282 electrons. The former projected to the normal of the lamellae in structure III have according to the calotte model of Fig. 1 a length of about 9.0 Å per molecule, the latter 16.5 Å. Therefore one obtains a mean density of 19.8 el. Å^{-1} and 17.1 el. Å^{-1} which differs only by about 13.5%. From Fig. 7 one learns therefore that this small relative fluctuation of $\varrho(x)$ is the reason for the large exposure times.

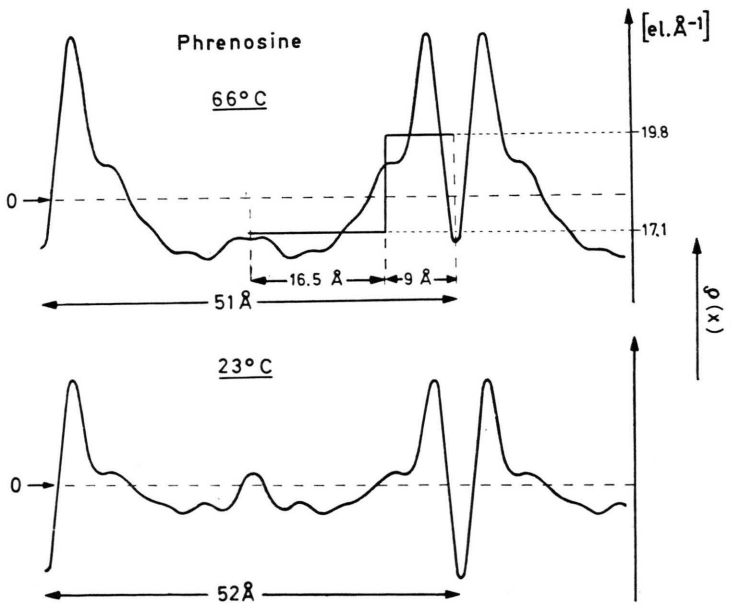

Fig. 7. Electron density projection $\varrho(x)$ of one bimolecule of structure II (23 °C) and III (66 °C) on the normal of the lamellae. The gap between two 9 Å thick galactose compounds is deeper at 23 °C. The weak maximum in the centre of the bimolecule indicates the overlapping of the two different long paraffin chains (see Figs 9 and 10).

VII. WAXS at 23 °C and 66 °C

The WAXS pattern obtained at 23 °C till down to the SAXS reflections $n = 6$, 7, 8 and 9 is drawn in Fig. 8. At 66 °C the pattern is practically the same, small changes are discussed below. The analysis of the strongest 6 WAXS reflections between $b = 0.2\ \text{Å}^{-1}$ and $0.35\ \text{Å}^{-1}$ is unique, if one assumes for simplicity that they have all the same shape. We used a Du Pont 310 curve resolver taking Lorentzian squared profiles. These six reflections cannot be attributed to one lattice type but only to the superposition of reflections of two different lattices. They can be analysed as orthorhombic (O) and triclinic

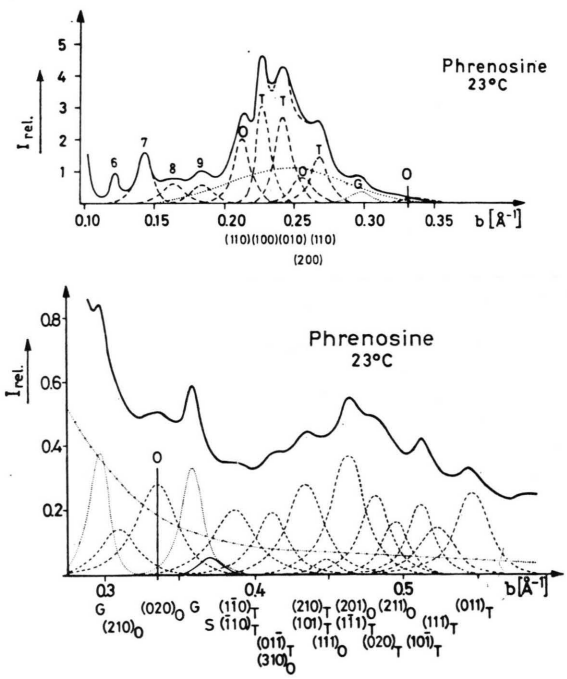

Fig. 8. WAXS of the orthorhombic (O) and triclinic (T) components of phrenosine at 23 °C and 66 °C. The dotted diffuse background together with the two reflections G is attributed to the galactose rings with amide-linkage. The reflections 6 to 9 are plotted in Fig. 6 too. The relative intensities from O to T are 40 : 60.

(T), if one compares their positions with well known paraffin lattices. The reflection at $b = 0.21$, 0.25, and $0.33\ \text{Å}^{-1}$ can be indexed as 110, 200, and 020 from type O and the three reflections at 0.23, 0.24, and $0.27\ \text{Å}^{-1}$ as 100, 010, and 110 from type T. From the relative intensities one learns moreover that type O is represented with ca. 40% and type T with ~60%.

Now the WAXS for $b > 0.35$ Å can be interpreted directly by the superposition of the other much weaker reflections of these two lattices. The single positions of these reflections are collected in Table III and compared with a calculated triclinic and orthorhombic lattice.

The agreement is quite satisfactory. The lattice constants are given in Table IV. The b-axis increases with rising temperature in the triclinic and decreases in the orthorhombic structure, where it becomes more hexagonal. The intensities remain unchanged.

It is interesting to note that the triclinic component has nearly the same lattice cell as the paraffin $C_{20}H_{42}$ [22]. The constants a and b have slightly changed from $a = 4.90$ Å and $b = 4.20$ Å *. The intensities of the reflections are also quite similar to $C_{20}H_{42}$.

The orthorhombic modification resembles C_nH_{2n+2} (with $n \geqq 26$) [23]. Only the volume of the lattice cell is somewhat larger than in these paraffins with $a \cong 7.4$ Å and $b \cong 4.9$ Å. This explains the large paracrystalline distortions of the mPC's discussed below. The relative intensities are surprisingly similar to those in polyethylene [24]. Obviously the 178 electrons of the heads are so randomly distributed that only two WAXS reflections are observable. They are labeled with G in Fig. 8 and Table III. Because these reflections give only a small contribution to the whole intensity, the rest of the diffraction of the heads must be sought in the diffuse background. The whole intensity (G-reflections + background) relative to the other reflections is given by the respective number of electrons, hence 178/282. With the help of this relationship the background is constructed in Fig. 8. The integral intensities of the triclinic reflections are in the ratio ~60 : 40 to the orthorhombic reflections according to Table V.

Now we can attribute both modifications of WAXS to the three strutures discussed from SAXS. From integral SAXS intensities at 23 °C we have calculated that 15% of the chains are in isolated MPC's of structure I (65 Å thick) and 85% in the bimodal structure II (52 Å thick). The latter consists of 26% statistically mixed lamellae ~60 Å thick with 74% lamellae of the 49 Å component.

* The triclinic subcell of Table IV differs from subcells used for fatty acid because instead of the b-axis of Table IV Chapmann [23] used a $(b-a)$-axis.

Table III. WAXS reflections of phrenosine. T, triclinic and O, orthorhombic component, G, reflection of galactose and the amide linkage, S, higher orders (n) from SAXS periodicity 49 Å at 23 °C and 50.8 Å at 66 °C.

Component	(hkl)	23 °C		66 °C	
		b_{exp} [Å^{-1}]	b_{calc} [Å^{-1}]	b_{exp} [Å^{-1}]	b_{calc} [Å^{-1}]
O	(110)	0.210	0.210	0.213	0.213
T	(100)	0.226	0.226	0.226	0.226
T	(010)	0.241	0.241	0.235	0.235
O	(200)	0.254	0.254	0.254	0.254
T	(110)	0.267	0.267	0.263	0.263
G		0.291	?	0.299	?
O	(210)	0.305	0.305	0.306	0.306
O	(020)	0.332	0.334	0.339	0.342
G		0.357	?	0.363	?
S	$n=18$	0.368	0.367		
T	$(1\bar{1}0)$	0.385	0.383	0.379	0.378
T	$(\bar{1}10)$				
S	$n=20$			0.392	0.394
T	$(01\bar{1})$	0.412	0.410	0.404	0.408
O	(310)		0.417	0.414	0.417
T	(210)	0.435	0.432	0.436	0.430
T	(101)		0.435		0.435
O	(111)	0.448	0.446	0.452	0.448
O	(201)	0.462	0.469	0.473	0.468
T	$(1\bar{1}1)$		0.470		0.468
T	(020)	0.481	0.482		0.471
O	(211)	0.494	0.498	0.490	0.498
T	$(10\bar{1})$	0.510	0.511	0.506	0.510
T	(111)	0.521	0.523	0.522	0.520
T	(011)	0.544	0.544	0.539	0.541

Table IV. Lattice cells of the two components of phrenosine.

	Triclinic		Orthorhombic	
	23 °C	66 °C	23 °C	66 °C
a	(4.73 ± 0.02) Å	(4.74 ± 0.02) Å	(7.85 ± 0.02) Å	(7.88 ± 0.03) Å
b	(4.60 ± 0.02) Å	(4.71 ± 0.02) Å	(5.98 ± 0.02) Å	(5.84 ± 0.03) Å
c	2.54 Å		2.54 Å	
α	106°		90°	
β	85°			
γ	72°			

Table V. Distribution of the two types of subcells with a long period P into the 3 structures.

	Orthorhombic		P	Triclinic	P
23 °C	I	15%	65 Å	—	—
	II	22%	65 Å	63%	49 Å
66 °C	III	37%	45 Å	63%	52 Å

This means in the whole sample one has 37% thicker lamellae of ~60 Å and 63% of 49 Å. This nicely corresponds with the WAXS-values and proves directly that structure I and the thicker lamellae of structure II have orthorhombic subcells whilst the 49 Å lamellae are triclinic (Table V).

At 66 °C in SAXS only structure III appears with 51 Å periodicity. Because the same ratio in WAXS between orthorhombic and triclinic chain packing is observed one must conclude that the chains of isolated structure I and of the ~60 Å component in structure II have tilted to a smaller angle between lamellae surface and chain direction but retained their orthorhombic subcell.

The next interesting finding is that the orthorhombic paraffins C_nH_{2n+2} (with even $n>26$) can be found in two different modifications with a tilt angle of 61° and 90° to the lamellae surface[25]. Since a double molecule of phrenosine has a length of 69 to 74 Å, depending on the tilt angle of the galactose ring to the chain direction, one obtains

for a 61° angle between chain and lamella-surface a lamella-distance of 60 to 64 Å. Using the calotte model of Fig. 1 one finds that for this 61° angle the galactose rings have no space for tilting the head. Then one comes to a periodicity of $P \sim 65$ Å which agrees nicely with the SAXS of structure I [see Eqn (3)]. The corresponding structure is drawn in Fig. 9.

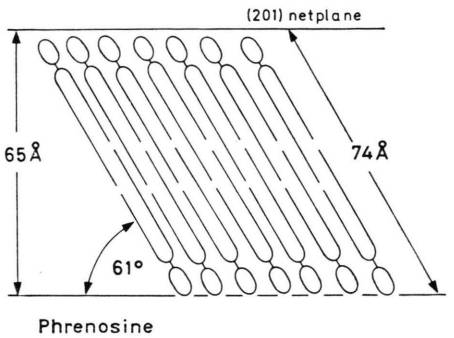

Fig. 9. The orthorhombic structure I and the component of thicker lamellae in structure II. The (201) netplanes of the subcell are parallel to the lamellae surface. The galactose heads are not inclined against the chain direction.

The netplanes (201) of the orthorhombic 61°-tilted paraffin chains are parallel to the lamellae surfaces. This also holds for the subcells of structure I. Another interesting point is that the (301)-netplanes of these paraffin chains have an angle of about 45° to the lamellae surface. This explains how at 66 °C structure I changes over to a part of structure III with a mean 51 Å periodicity. Now one gets for the periodicity $(69 \text{ to } 74)/\sqrt{2} = 49$ to 52 Å.

Since structure III consists of a mixture of those lamellae with triclinic lamellae and a mean $\overline{P} =$ 51 Å, the heads of the orthorhombic component obviously are still practically not tilted to the chain direction because the triclinic component with $P =$ 49 Å in structure II has strongly tilted heads (Fig. 10) and the average of 49 Å and the highest possible value 52 Å of the orthorhombic component gives the observed $\overline{P} = 51$ Å. If on the other hand the tilting of the galactose rings of the triclinic component is smaller at 66 °C, then the heads of the component may have some tendency of tilting their heads also because the 45° angle gives more space for tilting than the 60°. The $\varrho(x)$ curves of Fig. 7 give heads with a width of about 9 Å, which corresponds more to the tilted galactose

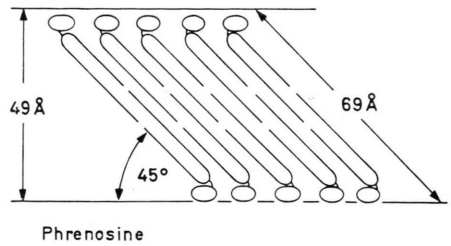

Fig. 10. The triclinic component of the thinner lamellae in structure II and the orthorhombic and triclinic components in structure III. Both have the same inclination of 45°. The (301) netplanes of the subcell of the orthorhombic component now are parallel to the lamellae surfaces. The tilt angle of their heads against the chain direction is perhaps smaller or eventually zero like in Fig. 9.

rings of Fig. 10, so perhaps the heads of the orthorhombic modification tilt also to some degree.

It is interesting to note that the lattice planes of the subcells obviously stabilize the whole structure in spite of the disturbing intermediate sheets of the heads. Their disturbing effects influence mainly the number of lamellae in the MPC. In paraffin with its well-defined methyl-endgroups the bundles are much larger and sometimes crystallographically aligned in such a way as to produce coherent WAXS over 30 or more lamellae [26]. In phrenosine the galactose heads disturb this coherency totally and that is why only 4 to 7 lamellae cluster together [Eqns (3) and (18)].

VIII. Size and Distortions of the mPC's

From SAXS studies we had obtained in section III till V the sizes of bundles of lamellae which were called MPC's. They had normal to the lamellae a size of 230 and 290 Å [Eqns (3) and (18)] and lateral dimensions somewhat larger resp. smaller [see Eqn (17)].

Analysing WAXS one obtains direct information about the lateral distances and lateral distance fluctuations of adjacent molecules and the size of paracrystalline domains, called mPC's, which these molecules build up. We find these mPC's everywhere in synthetic polymers. To prove their paracrystalline nature one has to analyse the line widths of at least 3 orders of one netplane in $\delta b - b^2$ diagrams analogous Fig. 4.

Unfortunately there exist only two orders of reflections in the case of (010) for the triclinic subcells at 23 °C. Applying the $\delta b - b^2$ plot one obtains

$$D_{010} = 45 \text{ Å}; \; g_{010} = 2.6\% \text{ (triclinic, 23 °C)}. \quad (22)$$

At 66 °C the 020 reflection is overlapped by two other reflections (Table IV) and the g-value of the subcells cannot be calculated. Nevertheless one can calculate the sizes D from only one order of reflections using an emperical formula which holds for many noncrystalline materials and combines the g-value with the number N of netplanes in one mPC [27]:

$$N = (\alpha^*/g)^2 . \tag{23}$$

With the values of Eqn (22) one finds for (010) triclinic at 23 °C

$$\alpha^* = 0.08 \tag{24}$$

which agrees nicely with other results. The α^* values of SAXS can be also calculated from Eqn (3) for the MPC of structure I. One finds again

$$\alpha^* = 0.08 . \tag{25}$$

Introducing Eqn (23) into Eqn (1) one finds for the first order reflections

$$\delta b = \frac{1}{a}\left[\frac{1}{N} + \left(\frac{\pi\alpha^*}{N}\right)^2\right] = \frac{1}{D}\left[1 + (\pi\alpha^*)^2\right] \tag{26}$$

(a, netplane distance; $\overline{D}$, size of mPC's). Assuming paracrystalline distortions of the same type as in the triclinic (010) in all other netplanes one can now calculate the size $\overline{D}$ of the mPC's in all other directions. This is done in Table VI. Sizes between 40 and 100 Å were found. This means that in the average each MPC, consisting of $N = 4$ to 7 double molecular lamellae [see Eqns (3), (15), and (18)] and a lateral size B of ~ 200 Å [see Eqn (17)], contains 16 or more mPC's with a mean lateral diameter between 40 and 100 Å. The mPC's of the orthorhombic modification O become reasonably contains 16 or more mPC's with a mean lateral smaller at 66 °C in [100] direction, the mPC's of the triclinic modification T grow in the direction orthogonal to (010) netplanes and become somewhat smaller orthogonal to (100) and (110) netplanes. This may be explained by a kind of "premelting" and recrystallization.

Table VI. Integral widths δb of some WAXS reflections of phrenosine and size $\overline{D}$ of the mPC's in the respective directions calculated from Eqn (26).

(hk0)	23 °C		66 °C	
	$\delta b \times 10^3$[Å^{-1}]	$\overline{D}$[Å]	$\delta b \times 10^3$[Å^{-1}]	$\overline{D}$[Å]
O (110)	15.8	67	14.9	71
O (200)	17.5	68	23.6	45
T (100)	10.8	98	13.4	79
T (110)	16.9	63	26.0	41
T (010)	23.7	45	15.1	70
T (020)	29.2			

Let us now discusses the paracrystalline nature of these small compounds:

Sadler *et al.* [28] and Dorset [29] explained distortions in single crystals of polyethylene and n-hexatriacontane by microstresses. It must be pointed out that these samples were grown by evaporation of solution on an uneven polymeric support. The WAXS analysis of free crystallized polyethylene single crystals proves unequivocally the existence of paracrystalline distortions [30], whilst in paraffins no microscresses occur [26]. There is no reason for microstresses because native phrenosine was not grown on disturbing supports. The α^* relation (23) important for all colloidic systems explains the existence of non-crystallizing microdomains by liquid-like distortions which especially for structure III are obvious because the size of the subcells of the orthorhombic modification is larger than for the corresponding paraffin. Here the chain molecules have many more conformational possibilities than in paraffins.

This variety of conformations does not exist in paraffin molecules because they are short and distortions can be extruded by annealing. The lateral sizes of the mPC's are therefore, according to the α^*-law [Eqn (23)] immeasurably large. Moreover their heads consist of methyl-groups and can align in the lamellar structure often with a crystallographic order so that 20 or more lamellae give coherent diffraction effects in the chain direction [26]. The galactose rings totally destroy this coherency. The MPC-bundles consist therefore of not more than 7 bilayers. The paracrystalline structure of stacks of single crystals of linear polyethylene on the other hand have some similarities with phrenosine: The chain segments between two backfolds are full of conformational distortions (kinds) and the backfolds give contacts between adjacent lamellae only to a certain degree, but not as good as the galactose rings in phrenosine.

One of us (S. Fernandez-Bermudez) is greatly indebted to the Alexander von Humboldt-Stiftung, Bonn-Bad Godesberg, which generously supported him by a grant.

We thank M. Martin-Lomas from the Instituto de Quimica Organica, Madrid, for preparing the samples and Dr. F. J. Baltá-Calleja, Prof. Dr. W. Kreutz for meliorating the text and Dr. P. Bond for his helpful advice.

[1] R. Hosemann and W. Kreutz, Naturwissensch. **12,** 298 [1966].
[2] W. Luzzati, Biological Membranes, (D. Chapman, Ed.), Acad. Press, London, 1968.
[3] A. Tardieu and V. Luzzati, J. Mol. Biol. **75,** 711 [1973].
[4] G. G. Shipley, Biological Membranes, **Vol. II,** p. 1 (D. Chapman and D. F. H. Wallach, Eds.), Academic Press, London, 1973.
[5] Y. K. Levine, Prog. Surf. Membr. Sci. **3,** 279 [1973].
[6] C. R. Worthington, Curr. Top. Bioenerg. **5,** 1 [1973].
[7] E. H. Pape, W. Menke, and R. Hosemann, Biophys. J. **14,** 221 [1974].
[8] A. E. Blaurock, J. Mol. Biol. **93,** 139 [1975].
[9] R. Henderson, J. Mol. Biol. **93,** 123 [1975].
[10] E. G. Lapetina, E. F. Soto, and E. De Robertis, J. Neurochem. **15,** 437 [1968].
[11] M. M. Rapport and L. Graf, Prog. Allergy **13,** 273 [1969].
[12] M. Martin-Lomas and D. Chapman, Chem. Phys. Lipids **10,** 152 [1973].
[13] J. O'Brian and G. Rouser, J. Lipid Research **5,** 339 [1964].
[14] J. O'Brian, D. L. Fillerup, and J. F. Mead, J. Lipid Res. **5,** 109 [1964].
[15] A. W. Clowes, R. J. Cherry, and D. Chapman, Biochim. Biophys. Acta **249,** 301 [1971].
[16] E. Reiss-Hudson, J. Mol. Biol. **25,** 363 [1967].
[17] S. Abrahamsson, I. Pascher, K. Larsson, and K. Karlsson, Chem. Phys. Lipids **8,** 152 [1972].
[18] H. E. Carter, J. Rothfus, and R. Gigg, J. Lipid Res. **2,** 228 [1961].
[19] R. Hosemann and S. N. Bagchi, Direct Analysis of Diffraction by Matter, North-Holland Publ. Comp., Amsterdam, 1962.
[20] R. Hosemann, D. Weick, W. Vogel, and N. Müller, Ber. Bunsenges. Phys. Chem. **78,** 1358 [1974].
[21] W. Lesslauer and J. K. Blasie, Biophys. J. **12,** 175 [1972].
[22] W. Pechhold, S. Blasenbrey, and S. Woerner, Koll. Z. u. Z. Polym. **189,** 14 [1963].
[23] D. Chapman, The Structure of Lipids, Methuen and Co. Ltd., 1965.
[24] P. Zugenmaier, Strukturuntersuchungen an partiell-kristallinem Polyäthylen und Äthylen-Propylen-Copolymeren, Dissertation, Freiburg i. Br., 1969.
[25] S. M. Ohlberg, J. Phys. Chem. **63,** 248 [1959].
[26] O. Phaovibul, H. Čačković, J. Loboda-Čačković, and R. Hosemann, J. Polymer Sci. (Phys.) **11,** 2377 [1973].
[27] R. Hosemann, CRC Crit. Rev. Macromol. Sci. **1,** 351 [1972].
[28] D. M. Sadler and A. Keller, Koll. Z. u. Z. Polym. **239,** 641 [1970].
[29] D. L. Dorset, Naturwissenschaften **62,** 343 [1975].
[30] R. Hosemann and W. Wilke, Makromol. Chem. **118,** 230 [1968].